Retrospective Study

A Nomogram to Predict of Epidural Blood Patch Treatment Failure in Patients With Spontaneous Intracranial Hypotension and Subdural Hematoma

Hua Huang, MD[1], Fei-Fang He, MD[1], Zhong-Feng Niu, MD[2], and Ting-Ting Wei, MD[3]

From: [1]Department of Pain Management, Center for Intracranial Hypotension Management, Sir Run Run Shaw Hospital, School of Medicine, Zhejiang University, Hangzhou, People's Republic of China; [2]Department of Radiology, Sir Run Run Shaw Hospital, School of Medicine, Zhejiang University, Hangzhou, People's Republic of China; [3]Department of Anesthesiology, Sir Run Run Shaw Hospital, School of Medicine, Zhejiang University, Hangzhou, People's Republic of China

Address Correspondence: Ting-Ting Wei, MD Department of Anesthesiology, Sir Run Run Shaw Hospital, School of Medicine, Zhejiang University, Hangzhou, People's Republic of China E-mail: 3317057@zju.edu.cn

Disclaimer: There was no external funding in the preparation of this article.

Conflict of interest: Each author certifies that he or she, or a member of his or her immediate family, has no commercial association (i.e., consultancies, stock ownership, equity interest, patent/licensing arrangements, etc.) that might pose a conflict of interest in connection with the submitted article.

Article received: 03-26-2025
Revised article received: 06-16-2025
Accepted for publication: 06-26-2025

Free full article: www.painphysicianjournal.com

Background: Subdural hematoma (SDH) is a frequent and serious complication of spontaneous intracranial hypotension (SIH), often requiring timely intervention. An epidural blood patch (EBP) is widely recognized as the preferred interventional treatment for SIH and its complications. However, treatment failure remains a concern, and predicting outcomes in patients with SIH and a concurrent SDH post EBP remains a clinical challenge.

Objectives: Our study aimed to develop and validate a predictive nomogram for treatment failure following an EBP in patients with SIH complicated by an SDH, identifying key clinical and imaging predictors associated with poor prognosis.

Study Design: This was a retrospective cohort study conducted over a 7-year period.

Setting: The study was conducted from January 2017 through December 2023 at a single tertiary care center, using electronic health records and radiologic databases.

Methods: A total of 233 patients diagnosed with SIH and concurrent SDH and treated with an EBP were retrospectively enrolled. Patients were sequentially assigned to a development cohort (n = 175) and a validation cohort (n = 58) at a 3:1 ratio. Backward stepwise multivariable logistic regression was applied to the development cohort to identify independent treatment failure predictors. A nomogram was constructed based on the final regression model. The model's performance was assessed through discrimination (C-index), calibration plots, and decision curve analysis to evaluate clinical utility.

Results: Treatment failure occurred in 86 of 233 patients (36.9%), with similar rates between development (36.6%) and validation (37.9%) cohorts ($P = 0.977$). Four independent predictors were identified: gender, the maximum SDH thickness, SDH density type (based on computed tomography brain imagery), and pontomesencephalic angle. Specifically, men (odds ratio [OR] = 2.63; 95% CI, 1.11–6.48; $P = 0.030$), greater SDH thickness (OR = 1.26 per mm increase; 95% CI, 1.13–1.43; $P < 0.001$), non-low-density SDH—including isodense, hyperdense, mixed-density, and layering patterns—(vs low-density; OR = 0.35; 95% CI, 0.14–0.88; $P = 0.025$), and smaller pontomesencephalic angle (OR = 0.95 per degree; 95% CI, 0.91–0.99; $P = 0.030$) were significantly associated with increased risk. The nomogram demonstrated strong discrimination in the development cohort (C-index = 0.87; 95% CI, 0.82–0.93) and maintained good performance in the validation cohort (C-index = 0.84; 95% CI, 0.73–0.94). Calibration was satisfactory in both cohorts, and a decision curve analysis confirmed the model's clinical value.

Limitations: While the sample size is the largest among similar studies, it remains relatively modest. Our exclusion of iatrogenic SIH and cases with cerebrospinal fluid fistulas may limit generalizability. Additionally, reliance on heavily T2-weighted magnetic resonance myelography without a reference standard for cerebrospinal fluid leak localization may affect generalizability. Prospective, multicenter trials are warranted to validate and refine the model.

Conclusions: Our study presents a validated nomogram incorporating 4 key predictors—

gender, SDH thickness, SDH density, and pontomesencephalic angle—that accurately estimates treatment failure risk following an EBP in patients with SIH and a concurrent SDH. This tool offers practical value for individualized risk assessment and clinical decision-making.

Key words: Nomogram, treatment failure, spontaneous intracranial hypotension, epidural blood patch, subdural hematoma

Pain Physician 2026: 29:E29-E42

Spontaneous intracranial hypotension (SIH) is a disorder caused by cerebrospinal fluid (CSF) leakage (1). Reduced CSF volume can trigger compensatory expansion of the subdural/subarachnoid spaces, resulting in subdural fluid accumulation and brain displacement, potentially causing tears in bridging veins and leading to a subdural hematoma (SDH) (2). An SDH is a potentially life-threatening complication in patients with SIH, occurring at a rate of approximately 20% to a maximum of 45% (3). In severe cases, patients with SIH and a concurrent SDH may experience neurological deficits, altered consciousness, and cerebral herniation, which may even lead to death (4).

Once SIH is diagnosed, prompt identification of the CSF leak site is essential (5). Precise localization of the leak is crucial for guiding treatment decisions, including targeted epidural blood patch (EBP) treatment or surgical repair. However, managing SIH complicated by an SDH is more challenging, as it requires addressing both the CSF leak and the associated hematoma. Surgical intervention for SDH may involve drainage, hematoma evacuation, or middle meningeal artery embolization (6,7). Nevertheless, the optimal management strategy for SIH with a concurrent SDH remains controversial.

Conservative therapy may be effective for patients with SIH and a concurrent SDH (8); however, in most cases, EBP therapy, surgical intervention, or a combination of both needs to be considered (3,7,9-11). While Chen, et al (2) indicated that early surgical intervention can prevent uncal herniation in patients with SIH and a concurrent SDH $\geq$ 10 mm and lower Glasgow Coma Scale scores (2), there are also reports suggesting that an EBP alone can achieve a cure for patients with SIH and a concurrent SDH, even if the SDH is thick (12).

Compared to surgery, EBP treatment is associated with lower risks, fewer adverse events, and significantly reduced recovery time and costs (13,14). However, patients with SIH and a concurrent SDH have a high failure rate following an EBP treatment, with some studies reporting rates as high as 37% (2,7). Treatment failure not only prolongs the disease course, but also increases the risk of severe complications associated with an SDH. Thus, distinguishing between patients who recover and those who fail, thus requiring further intervention, is critical for optimizing treatment outcomes. Our study aimed to develop and validate a nomogram that integrates multiple independent predictors to provide an accurate and user-friendly tool for predicting treatment failure in patients with SIH and concurrent SDH treated with an EBP.

Methods

Patients

Our retrospective study was approved by the institutional ethics committee (No. 2023-745-01). Given the retrospective nature of the study, the ethics committee of our hospital waived the need for informed consent from patients. This work was in line with the Strengthening The Report Of Cohort Studies in Surgery (STROCSS) criteria (2024 version) (15).

No statistical power calculation was conducted prior to the study. The sample size was determined based on the available data from our institutional clinical database collected from January 2017 through December 2023. We reviewed the clinical databases of 305 patients diagnosed with SIH and concurrent SDH during this period. The diagnosis of SIH was based on the criteria from the International Classification of Headache Disorders, Third Edition (ICHD-3, code 7.2.3): low CSF pressure (< 60 mm CSF) or imaging evidence of CSF leakage; headaches occurring in temporal relation to low CSF pressure or CSF leakage; or headaches not better explained by another diagnosis (16). An SDH was defined as a blood collection between the dura mater and the arachnoid membrane in the cranial cavity as seen on brain computed tomography (CT), in either chronic or mixed form.

The inclusion criterion was all patients with SIH with a concurrent SDH who underwent an EBP treatment.

The exclusion criteria were: 1) an absence of a CSF

leak on heavily T2-weighted magnetic resonance myelography (HT2W-MRM); 2) intracranial hypotension secondary to post dural puncture (meeting ICHD-3 criteria and occurring within 5 days of the puncture) or a CSF fistula (meeting ICHD-3 criteria and developing in temporal relation to a procedure or trauma); 3) an EBP treatment, fibrin patching, or endovascular sealing before hospital admission; 4) surgical interventions (including drainage, SDH evacuation, or middle meningeal artery embolization) before an EBP treatment; and 5) incomplete data. No predefined protocol determined the priority between conservative treatment and surgical intervention for a SDH. The decision for surgical intervention was made through consensus among the attending neurologist or neurosurgeon and the patient/family. Patient data were anonymized.

Demographics and Clinical Profiles

Demographic characteristics and clinical variables were collected, including gender, age, height, weight, body mass index (kg/m^2), smoking status, and a history of connective tissue disease, hypertension, and diabetes. Other recorded factors included a history of intrathecal anesthesia; misdiagnosis; clinical presentations such as headache intensity (measured on a 0-10 Numeric Rating Scale, with scores obtained the day before EBP treatment); nausea or vomiting; visual symptoms; auditory symptoms; neck pain or stiffness associated with this syndrome; time from onset to diagnosis; times of EBP treatment; total volume of autologous blood injected into the epidural space; and overall length of hospital stay. Notably, in all patients with a history of intrathecal anesthesia, the onset of symptoms related to intracranial hypotension occurred more than 5 days post dural puncture, suggesting a delayed presentation inconsistent with typical post dural puncture headache.

Neuroimaging

Pre-EBP brain CT, brain magnetic resonance imaging (MRI), and HT2W-MRM were also analyzed. In cases where a patient underwent multiple pre-EBP CT, MRI, or HT2W-MRM scans, the most recent scan, closest to the time just before the first EBP treatment, was selected for analysis.

Brain CT was performed to record the SDH laterality, the maximum thickness of SDH (MTH), the sum of the maximum SDH thicknesses on both sides, SDH density type, and midline shift. MTH was defined as the greatest axial diameter of the hematoma measured on either side of the brain CT and was recorded in millimeters. The SDH on CT scans was classified into 2 categories: low-density SDH and non-low-density SDH. Low-density SDH appeared as hypodense on brain CT, whereas non-low-density SDH included isodense, hyperdense, mixed-density, and layering patterns (17) (Fig. 1).

The following brain MRI signs were recorded: iter descent below the incisural line (> 1.8 mm) (18); intracranial angle, including pontomesencephalic angle1 (PMA) (19) and the angle between the vein of Galen and straight sinus (vG/SS angle) (20); downward displacement of the cerebellar tonsils (21); and pituitary hyperemia (22). HT2W-MRM identified the location of CSF leaks and the presence of high cervical (C1-C2 to C2-C3) leaks. A CSF leak was confirmed if a fluid-equivalent signal was detected in the epidural or perineural space. The length of periradicular leaks was measured using vertebral segments (23).

Although CT myelography remains the gold standard for detecting CSF leakage, it carries inherent risks, including invasiveness, radiation exposure, and allergic reactions to iodine-based contrast agents (24). Studies have shown that HT2W-MRM can detect CSF leakage with an accuracy of up to 93.5%, demonstrating excel-

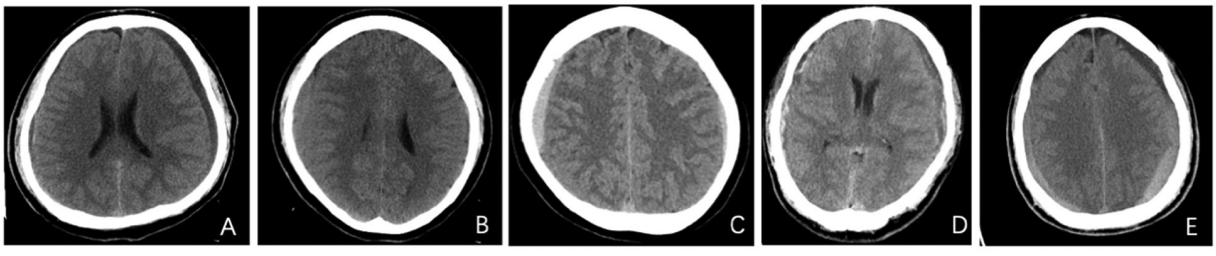

Fig. 1. *CT scans illustrating 5 distinct types of subdural hematoma: (A) low-density, (B) isodensity, (C) high-density, (D) mixed-density, and (E) layering.*

lent concordance with CT myelography (25,26). As a noninvasive and radiation-free modality, HT2W-MRM serves as a viable alternative for diagnosing SIH. Therefore, HT2W-MRM was used in this study to identify CSF leakage. Some MRI or HT2W-MRM measurements are shown in Fig. 2. Demographic, clinical, and imaging parameters were collected based on previous studies on the treatment failure of SIH (3,9,21,23,27-29), as well as our own clinical experience. All imaging findings were jointly obtained by 2 experienced neuroradiologists who were unaware of the patient's identity.

Intervention and Outcomes Analyses

EBP target sites were selected based on their CSF leak level, as identified by HT2W-MRM (30). EBP was administered at the identified leak site, the center of the segmental leak, or 2 locations to adequately cover diffuse or multifocal leaks. Based on clinical experience, for patients with no significant symptom relief within 72 hours post EBP treatment or those displaying multiple-segment CSF leaks on HT2W-MRM, we conducted additional or repeated EBP sessions at intervals of 3–5 days. We recorded the number of EBP treatments performed during the same hospital admission, as well as the total volume of autologous blood injected into the epidural space.

Treatment failure was defined as the persistence or partial relief of symptoms (< 30% decrease in headache intensity [31,32]), or progression of the SDH. In addition, EBP treatment was deemed a failure if readmission for the same condition occurred within 6 months postdischarge, regardless of the patient's assessed efficacy.

Statistical Analysis

Continuous data are presented as mean ± SD for normally distributed variables, or median with interquartile range (IQR) for nonnormally distributed vari-

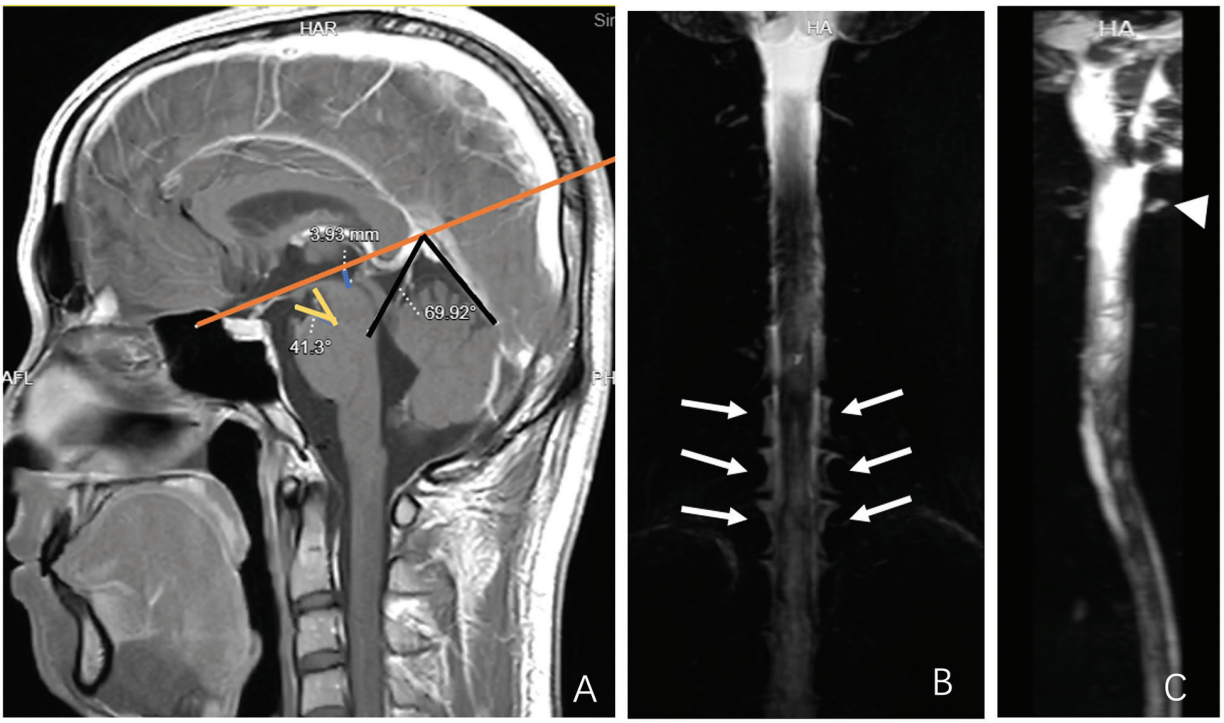

Fig. 2. *MRI and HT2W-MRM showing measurements of anatomical angles and locations of spinal CSF leak. (A) Black lines show the vG/SS angle. The blue line indicates the distance from the opening of the sylvian aqueduct (i.e., iter) to the incisural line (the orange line starts from the anterior tuberculum sellae and passes through the junction of the great cerebral vein, inferior sagittal sinus, and straight sinus). Yellow lines denote PMA, which was defined as the angle between the line tangential to the anterior margin of the midbrain and the line tangential to the superior margin of the pons based on the midline sagittal view of the brain MRI. (B) HT2W-MRM imaging shows the CSF leak at the cervicothoracic junction (arrow). (C) HT2W-MRM imaging of the spine shows abnormal CSF signals in the high cervical region (C1–C2 to C2–C3) (arrowhead).*

ables. Normality was assessed using the Shapiro-Wilk test. Categorical data are presented as counts and percentages. Differences in continuous variables were assessed using the Mann-Whitney U test, as none met the normality assumption. Categorical variables were compared using the χ^2 test or Fisher's exact test, as appropriate. Spearman correlation and the Belsley collinearity test were used to evaluate collinearity among all covariates. A condition index threshold of 30 was used to indicate potential multicollinearity, and covariates with variance decomposition proportions greater than 0.5 were further examined. No significant multicollinearity issues were detected among the covariates included.

The significance of each variable in the development cohort was first evaluated through univariate logistic regression analysis in order to identify potential risk factors for treatment failure. Clinically relevant variables and those with a P value < 0.1 in the univariate analysis were included in the multivariable logistic regression analysis. A backward stepwise elimination procedure, guided by the Akaike Information Criterion, was used to derive the final reduced model. Variables were removed sequentially if their contribution to the model did not meet the predefined threshold, ensuring a balance between model simplicity and predictive accuracy. Importantly, no variables were intentionally excluded for reasons outside the statistical procedure. Estimated odds ratios (OR) and 95% CIs were reported for the predictors in the final model.

A nomogram was then constructed based on the coefficients obtained from the reduced multivariable logistic regression model, scaling the regression coefficients to create a point-based scoring system that reflects the relative contribution of each predictor to the outcome. The coefficients from the regression analysis were scaled by dividing each coefficient by the smallest coefficient in the model and then rounding to the nearest whole number to create a point-based scoring system. Each predictor in the nomogram was assigned a corresponding point value proportional to its scaled coefficient, reflecting its relative contribution to the outcome. To use the nomogram, a vertical line was drawn from the value of each predictor to the point axis to determine its assigned score. The total score was then calculated by summing the points from all predictors. Finally, a vertical line was drawn from the total points axis to the risk axis to estimate the probability of failure.

We utilized the area under the curve (AUC) of the receiver operating characteristic (ROC) curve analysis and concordance index (C-index) to evaluate the nomogram's discrimination in predicting patient outcomes. The optimal cutoff for the model was determined using the Youden Index, which maximizes the sum of sensitivity and specificity. At the established cutoff, various performance metrics, including accuracy; sensitivity; specificity; positive and negative likelihood ratios; as well as positive and negative predictive values were calculated for both the development and validation cohorts. The best-fit model and nomogram were validated and calibrated using bootstrapping techniques. The bootstrap method was applied with 1,000 resamples, and the bootstrap-corrected AUC with a 95% CI was reported. Calibration plots of the nomogram were evaluated using the Hosmer-Lemeshow test. Additionally, a decision curve analysis was conducted to assess the net benefit of using the nomogram for predicting treatment failure across different threshold probabilities in both the development and the validation cohort.

All statistical analyses were conducted using R version 4.3.2 (The R Foundation) within the RStudio 2023.09.1 environment (Posit Software PBC). For model development and assessment, the following R packages were utilized: rms (version 6.9.0), caret (version 7.0.1), and pROC (version 1.18.5). These packages were used for constructing the nomogram, evaluating the model performance, and determining the optimal cutoff, respectively. Statistical testing was two-tailed and considered significant at $P < 0.05$.

Results

Patient Characteristics and Variables

A total of 305 patients with SIH and concurrent SDH were screened, of which 233 met the inclusion criteria and completed follow-up. Of the 72 excluded patients, 5 resulted from post dural puncture or CSF fistula, 13 had no significant CSF leak seen on HT2-MRM, 11 had an EBP treatment prior to admission, 11 underwent surgery first, and 32 had missing data (Fig. 3). Missing data accounted for 10.5% of the total screened patients. Sensitivity analyses confirmed that the excluded patients with missing data did not differ significantly in baseline characteristics compared to the included cohort.

Ultimately, A total of 233 patients were included, with 175 assigned to the development cohort and 58 to the validation cohort, maintaining a 3:1 ratio. This splitting was performed without replacement using

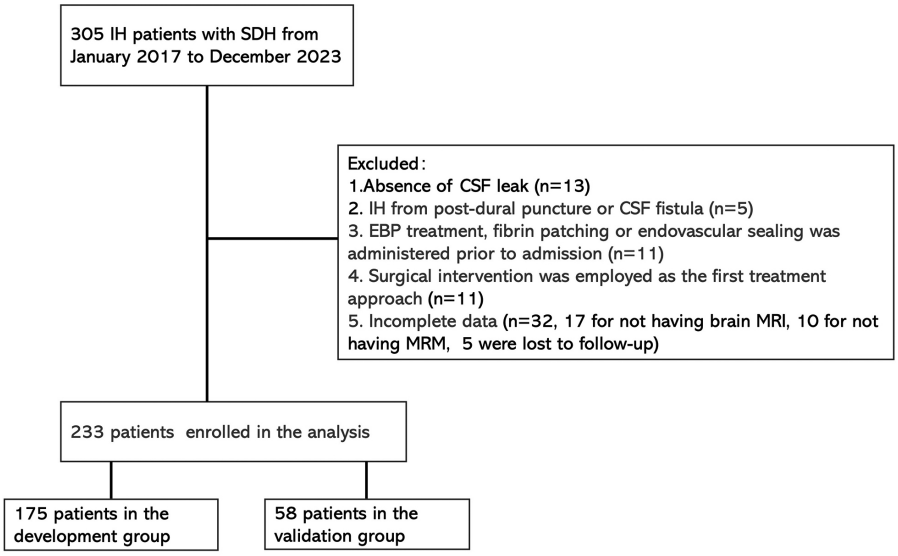

Fig. 3. *Flow diagram of the study population.*

a sequential approach, based on the order of patient admissions over the study period. As shown in Table 1, there were no significant differences in demographic, clinical, or imaging characteristics between the 2 cohorts. The median age at onset was 43 years, with a slight predominance of men (55.4%). The total number of treatment failures was 86 (36.9%), with 64 (36.6%) in the development cohort and 22 (37.9%) in the validation cohort.

Three patients (1.3%) in the enrolled population were diagnosed with connective tissue disease, all of whom were in the development cohort. Nausea or vomiting was the most prevalent onset feature (64.4%), followed by auditory symptoms (48.5%) and neck pain or stiffness (40.8%), with visual symptoms (14.2%) being less common. The median time from symptom occurrence to diagnosis was 45.0 days (IQR, 25.0–60.0). Before the correct diagnosis, 47 patients (26.9%) in the development cohort and 12 patients (20.7%) in the validation cohort were misdiagnosed. Bilateral SDHs were observed in 194 patients (83.3%), with 145 (82.9%) in the development cohort and 49 (84.5%) in the validation cohort. Additionally, 147 patients (63.1%) had a low-density SDH, including 114 (65.1%) in the development cohort and 33 (56.9%) in the validation cohort. Most CSF leakage sites were in the cervical and thoracic segments, with 176 (75.5%) involving cervical and cervicothoracic junctions and 168 (72.1%) involving thoracic and thoracolumbar junctions; lumbar CSF leakage was relatively rare, observed in only 68 patients (29.2%).

Nomogram Model Development

In a univariate regression analysis, variables with $P < 0.1$ included gender, a history of intraspinal anesthesia, nausea/vomiting, neck pain/stiffness, MTH, sum of the maximum SDH thicknesses on both sides, low-density SDH, midline shift, iter descent below the incisural line (> 1.8 mm), PMA, vG/ss angle, periradicular leak length, thoracic-thoracolumbar leak, and length of hospital stay. The results, along with their estimated OR and 95% CI, are presented in Table 2. The covariates obtained after backward multivariable regression were gender, a history of intraspinal anesthesia, neck pain/stiffness, MTH, low-density SDH, and PMA. Variables such as a history of intraspinal anesthesia and neck pain/stiffness were removed from the multivariable logistic regression analysis as they did not show statistical significance ($P > 0.05$).

After conducting multivariable logistic regression analysis, which adjusted for potential confounding variables, the independent predictors identified were gender, MTH, low-density SDH, and PMA (Table 2). Men (OR, 2.63; 95% CI, 1.11–6.48; $P = 0.030$) and greater MTH (OR, 1.26; 95% CI, 1.13–1.43; $P < 0.001$) were associated with a higher likelihood of treatment failure. In contrast, low-density SDH (OR, 0.35; 95% CI, 0.14–0.88; $P = 0.025$) and a smaller PMA (OR, 0.95; 95% CI,

Table 1. *Patient characteristics*.

Characteristics	Total (n = 233)	Development Cohort (n = 175)	Validation Cohort (n = 58)	*P*
Treatment failure, n (%)	86 (36.9%)	64 (36.6%)	22 (37.9%)	0.977
Gender (men), n (%)	129 (55.4%)	96 (54.9%)	33 (56.9%)	0.906
Age, years; median (IQR)	43.0 (35.0-54.0)	43.0 (35.0-52.5)	44.5 (35.0-54.0)	0.919
Height, cm; median (IQR)	167.0 (160.0-172.0)	167.0 (160.0-172.0)	168.5 (162.3-174.0)	0.101
Weight, kg; median (IQR)	65.0 (55.0-71.0)	64.0 (55.0-71.0)	65.0(55.0-70.8)	0.927
BMI, kg/m^2; median (IQR)	22.8 (20.8-25.3)	22.9 (20.8-25.3)	22.5(20.3-24.2)	0.303
Smoker, n (%)	27 (11.6%)	19 (10.9%)	8 (13.8%)	0.712
Connective tissue disorder, n (%)	3 (1.3%)	3 (1.7%)	0 (0%)	0.576
Hypertension, n (%)	50 (21.5%)	38 (21.7%)	12 (20.7%)	> 0.999
Diabetes, n (%)	24 (10.3%)	20 (11.4%)	4 (6.9%)	0.456
History of intrathecal anesthesia, n (%)	61 (26.2%)	44 (25.1%)	17 (29.3%)	0.650
Misdiagnosis, n (%)	59 (25.3%)	47 (26.9%)	12 (20.7%)	0.446
Headache intensity, scores; median (IQR)	2.0 (1.0-3.0)	2.0(1.0-3.0)	2.0 (1.0-3.0)	0.692
Nausea/vomiting, n (%)	150 (64.4%)	113 (64.6%)	37 (63.8%)	> 0.999
Visual symptoms, n (%)	33 (14.2%)	22 (12.6%)	11 (19%)	0.321
Auditory symptoms, n (%)	113 (48.5%)	91 (52.0%)	22 (37.9%)	0.088
Neck pain/stiffness, n (%)	95 (40.8%)	75 (42.9%)	20 (34.5%)	0.332
TOD, days; median (IQR)	45.0 (25.0-60.0)	45.0 (25.0-60.0)	45.0 (25.0-60.0)	0.814
NOE, number; median (IQR)	51.0 (33.0-68.0)	51.0 (34.0-67.5)	50.0 (30.8-77.3)	0.975
Volume of injected blood, mL; median (IQR)	22.0 (17.0-33.0)	23.0 (16.5-35.0)	19.0 (17.0-29.8)	0.265
LOS, days; median (IQR)	15.0 (12.0-20.0)	15.0 (12.0-21.0)	14.0 (11.0-19.0)	0.104
CT Signs				
Bilateral SDH, n (%)	194 (83.3%)	145 (82.9%)	49 (84.5%)	0.933
MTH, mm; median (IQR)	5.4 (3.3-9.7)	5.4 (3.2-8.8)	6.5 (3.6-10.9)	0.193
Sum of bilateral SDH, mm; median (IQR)	8.2 (5.4-14.8)	8.0 (5.2-14.6)	9.4 (6.2-16.4)	0.184
Low density SDH, n (%)	147 (63.1%)	114 (65.1%)	33 (56.9%)	0.332
Midline shift, n (%)	44 (18.9%)	33 (18.9%)	11 (19%)	>0.999
MRI Signs				
Iter > 1.8 mm below incisura line, n (%)	86 (36.9%)	65 (37.1%)	21 (36.2%)	>0.999
PMA, degree; median (IQR)	36.0 (29.5-42.1)	36.2 (29.7-42.0)	35.8 (28.6-42.6)	0.850
vG/ss angle, degree; median (IQR)	73.4 (64.1-81.3)	73.7(63.0-80.9)	73.2 (65.0-83.9)	0.184
Downward displacement of cerebellar tonsils, n (%)	8 (3.4%)	6 (3.4%)	2 (3.4%)	>0.999
Pituitary hyperemia, n (%)	161 (69.1%)	127 (72.6%)	34 (58.6%)	0.067
HT2W-MRM signs				
CSF leak location				
C-CT leak, n (%)	176 (75.5%)	135 (77.1%)	41 (70.7%)	0.415
T-TL leak, n (%)	168 (72.1%)	122 (69.7%)	46 (79.3%)	0.214
Lumbar leak, n (%)	68 (29.2%)	52 (29.7%)	16 (27.6%)	0.887
High cervical level CSF leakage, n (%)	99 (42.5%)	77 (44.0%)	22 (37.9%)	0.511
Periradicular leak length, median (IQR), n	7.0 (4.0-12.0)	8.0 (4.0-12.0)	7.0 (5.0-11.8)	0.796

Data are number (%), median (IQR (interquartile range)). TOD: time from onset to diagnosis; NOE: number of epidural blood patch treatment; LOS: length of hospital stays; SDH: subdural hematoma; MTH: maximum thickness of subdural hematoma; PMA: pontomesencephalic angle; vG/SS angle: angle between the vein of Galen and straight sinus; C-CT: cervical-cervicothoracic; T-TL: thoracic-thoracolumbar; CSF: cerebrospinal fluid.

Table 2. *Treatment failure risk factors.*

Characteristics	Univariate Analysis			Multivariable Analysis		
	OR	95% CI	*P*	OR	95% CI	*P*
Gender (men)	2.79	1.47-5.44	0.002*	2.63	1.11-6.48	0.030*
Age	1.00	0.98-1.03	0.739			
Height	1.02	0.99-1.06	0.237			
Weight	1.00	0.97-1.02	0.807			
BMI	0.96	0.87-1.05	0.366			
Smoker	1.65	0.62-4.34	0.304			
Connective tissue disorder	0.87	0.04-9.21	0.907			
Hypertension	1.02	0.47-2.12	0.969			
Diabetes	1.49	0.57-3.81	0.408			
History of intrathecal anesthesia	2.12	1.06-4.27	0.034*	2.29	0.89-6.01	0.086
Misdiagnosis	1.25	0.62-2.48	0.522			
Headache intensity	1.04	0.84-1.28	0.742			
Nausea/vomiting	0.46	0.24-0.87	0.017*			
Visual symptoms	0.61	0.21-1.59	0.336			
Auditory symptoms	0.66	0.35-1.21	0.180			
Neck pain/stiffness	0.46	0.24-0.88	0.019*	0.49	0.21-1.12	0.096
TOD	1.00	1.00-1.01	0.743			
NOE	1.00	1.00-1.01	0.623			
Volume of injected blood	1.00	0.97-1.02	0.680			
LOS	1.04	1.01-1.08	0.020*			
CT Signs						
Bilateral SDH	0.60	0.27-1.35	0.210			
MTH	1.38	1.25-1.56	< 0.001*	1.26	1.13-1.43	<0.001*
Sum of bilateral SDH	1.23	1.15-1.32	< 0.001*			
Low-density SDH	0.11	0.05-0.22	< 0.001*	0.35	0.14-0.88	0.025*
Midline shift	5.67	2.54-3.45	< 0.001*			
MRI signs						
Iter > 1.8mm below incisura line	2.36	1.25-4.50	0.008*			
PMA	0.93	0.90-0.96	< 0.001*	0.95	0.91-0.99	0.030*
vG/ss angle	0.96	0.93-0.99	0.003*			
Downward displacement of cerebellar tonsils	1.77	0.32-9.82	0.492			
Pituitary hyperemia	0.58	0.30-1.15	0.120			
HT2W-MRM signs						
CSF leak location						
C-CT leak	0.63	0.31-1.30	0.210			
T-TL leak	0.26	0.13-0.51	< 0.001*			
Lumbar leak	1.12	0.57-2.18	0.736			
High cervical level CSF leakage	0.59	0.31-1.11	0.104			
Periradicular leak length	0.90	0.84-0.96	0.001*			

TOD: time from onset to diagnosis; NOE: number of epidural blood patch treatment; LOS: length of hospital stays; SDH: subdural hematoma; MTH: maximum thickness of subdural hematoma; PMA: pontomesencephalic angle; vG/SS angle: angle between the vein of Galen and straight sinus; C-CT: cervical-cervicothoracic; T-TL: thoracic-thoracolumbar; CSF: cerebrospinal fluid.
*The asterisk indicates that the variable was statistically significant.

0.91–0.99; $P = 0.030$) were linked to a reduced risk of treatment failure.

The nomogram incorporating these predictors was developed (Fig. 4). To obtain the predicted probability, the patient's gender, MTH, low-density SDH, and PMA are mapped onto the nomogram's axes. A vertical line was drawn to determine the score for each variable. The individual probability of treatment failure can be determined by summing the scores for all variables and identifying the corresponding total on the total points line.

Nomogram Model Validation

Our model demonstrated high precision using the bootstrap method in the development cohort, with a C-index of 0.87 (95% CI, 0.82–0.93). The Hosmer–Lemeshow test indicated no significant lack of fit ($P = 0.732$), confirming the model's predictive accuracy in the development cohort. Calibration plots showed a strong agreement between predicted and observed failure rates (Fig. 5A). In the validation cohort, the nomogram achieved a C-index of 0.84 (95% CI, 0.73–0.94) with reliable calibration (Fig. 5B), as evidenced by the Hosmer–Lemeshow test, which also showed no significant variance (*P*

= 0.306). The correspondent ROC curve and its AUC of the development cohort and validation cohort for the nomogram are displayed in Fig. 6.

Treatment Failure Risk Based on the Nomogram Scores

The optimal cutoff for the nomogram was 0.26 and 0.52 for the development and the validation cohort, respectively. The sensitivity, specificity, positive predictive value, negative predictive value, positive likelihood ratio, and negative likelihood ratio for distinguishing between the presence and absence of failure were 64.71%, 90.00%, 85.94%, 72.97%, 6.47 and 0.39 in the development cohort, and 73.91%, 85.71%, 77.27%, 83.33%, 5.17, and 0.30 in the validation cohort, respectively.

Clinical Use

The decision curve analysis for both the development and validation cohorts (Figs. 7A and 7B) demonstrates that the nomogram is effective in predicting treatment failure when the threshold probability for either the patient or physician ranges from 10% to 90%. This approach offers significantly more clinical benefit compared to either indiscriminate application or no use of the nomogram.

Discussion

In our study, the treatment failure rate for patients with SIH and concurrent SDH treated with an EBP was 36.9%, which closely aligned with the 37.1% and 37.0% reported in 2 other studies involving 35 and 27 patients with SIH and concurrent SDH who were treated with an EBP (2,7). This suggests that patients with SIH and concurrent SDH treated with an EBP have a high failure rate, underscoring the need for further research in order to improve a patient's prognosis. Although this is a single-center study, the treatment outcomes align with those reported in other regions, supporting the reliability and generalizability of our findings.

Regarding clinical indicators, few studies have addressed the prognosis of patients with SIH and concurrent SDH treated with an EBP. According to Hong, et al (27), being a man; having a history of regular smoking and alcohol consumption; having a headache occurring in the temporal position; a prolonged duration of symptoms; and a greater frequency of EBPs were identified as factors associated with the necessity for surgical intervention in patients with SIH and concurrent SDH. In a cohort study on gender differences in SIH, Po-Tso

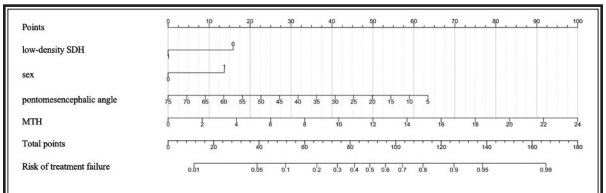

Fig. 4. *Established nomogram for the prediction of treatment failure of patients with SIH and concurrent SDH post epidural blood patch. The nomogram was developed by incorporating the following 4 parameters: low-density SDH on the brain CT, gender (men = 1, women = 0), pontomesencephalic angle (degrees), and MTH (mm). MTH: maximum thickness of subdural hematoma.*

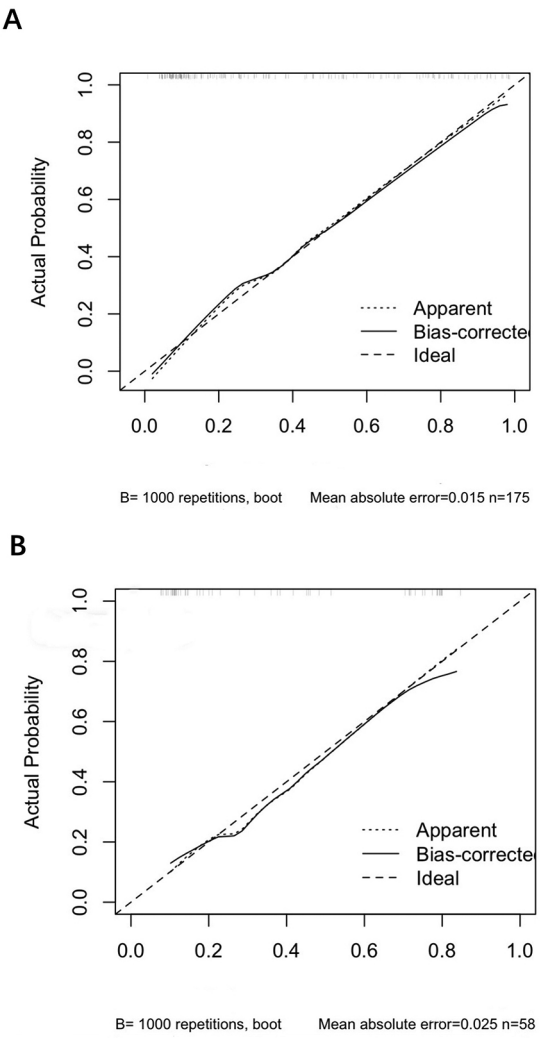

Fig. 5. *Calibration plot for nomogram in the (A) development cohort and (B) validation cohort.*

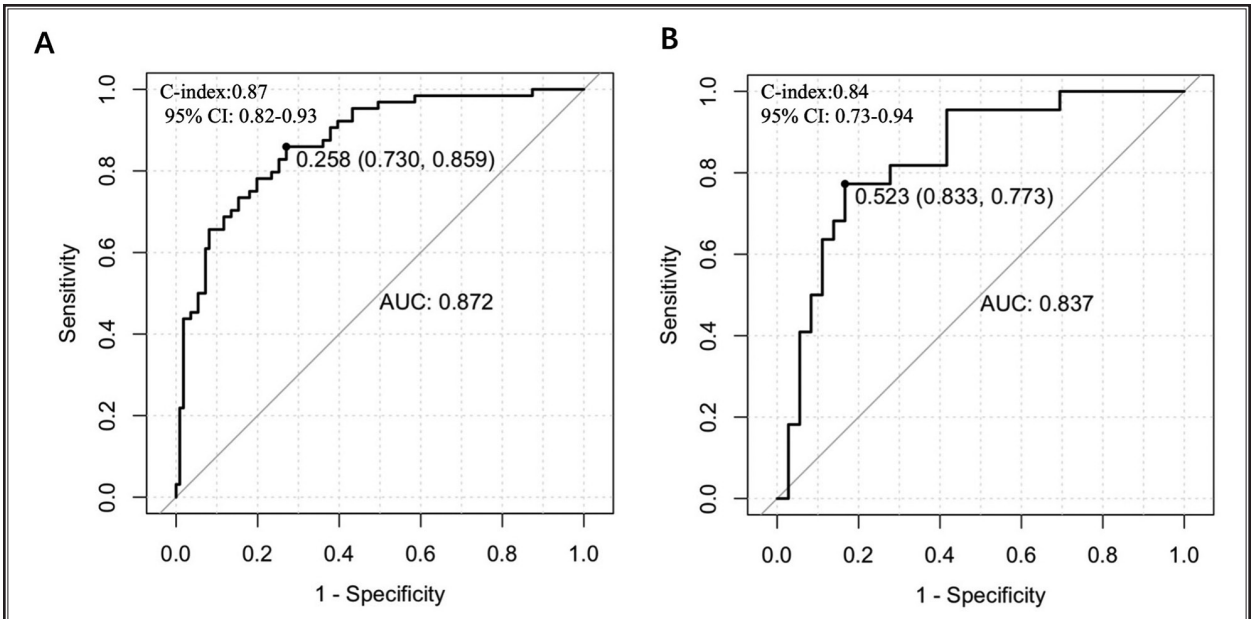

Fig. 6. *Receiver operating characteristic curve analyses of predictors for treatment failure in the (A) development cohort and (B) validation cohort.*

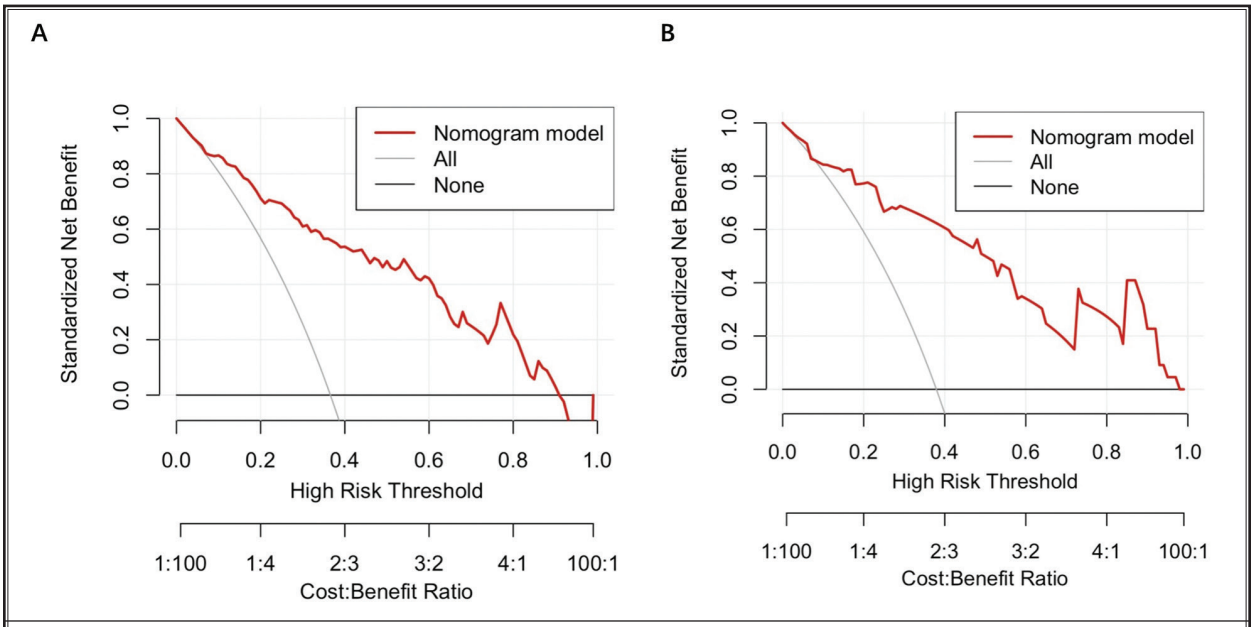

Fig. 7. *Decision curve analysis of treatment failure in patients with the nomogram model in the (A) development cohort and (B) validation cohort.*

Lin, et al (33) found that men had a higher risk of developing a SDH and were more likely to receive surgical drainage, which is consistent with our findings. While preliminary studies have investigated the relationship between gender and SIH, the available data remain limited, especially from multicenter, large-scale studies. Future research is needed to examine the specific effect of gender on pathogenesis, clinical presentation, prognosis, and treatment response in patients with SIH.

Our results also show that patients with SIH with

a large MTH had a higher risk of treatment failure after an EBP. Numerous studies have explored the effect of SDH thickness on the prognosis of chronic SDH. Increased SDH thickness is associated with a higher risk of treatment failure, and may even lead to acute postoperative neurological deterioration or brain herniation (2,34-38). According to the guidelines of Bullock, et al (39), for the surgical management of acute traumatic SDH, hematomas with a thickness ≥ 10 mm on CT scans should be promptly evacuated, regardless of the patient's Glasgow Coma Scale score. Some studies have also suggested that surgical intervention should be considered for patients with an SDH resulting from an SIH when the MTH is ≥ 10 mm (40). However, in clinical practice, we have observed that some patients with SIH and concurrent SDH ≥ 10 mm in thickness can be effectively managed with EBP therapy, obviating the need for surgical intervention, which is consistent with findings in other reported studies (7,10,41). Therefore, we propose that hematoma thickness may not be an exclusive determinant of the prognosis for patients with SIH and concurrent SDH undergoing EBP treatment. By quantifying the MTH along with other factors collectively influencing a prognosis and integrating them based on their contribution to the outcome, the resulting estimate of treatment failure risk may aid clinicians in making informed decisions for this specific patient subset.

Prior studies have explored the link between SDH density type and outcomes. In a retrospective study of 328 patients, Liu, et al (42) found that mixed-density SDH is an independent risk factor for treatment failure. Similarly, Yan, et al (43) reviewed data from 514 patients with chronic SDH and found high- and mixed-density SDHs to be significantly associated with treatment failure after burr hole surgery. Nakamura, et al (44) reported that every chronic SDH that resolved without surgery exhibited low density on follow-up CT scans. This study demonstrates an association between hematoma density and the prognosis of a SDH in patients with SIH. Our findings suggest that low-density SDH is associated with a reduced risk of treatment failure in patients with SIH following EBP therapy.

This study identified PMA as a significant predictor of treatment failure post EBP in patients with SIH and concurrent SDH. A smaller PMA is associated with a higher likelihood of treatment failure. One study indicated that individuals diagnosed with SIH and a PMA < 40° may be at a higher risk of treatment failure following an EBP (23). In a case-control study, Seung Hyun Lee, et al (45) found that patients with recurrent SIH who were treated with an EBP had a decreased PMA compared to the nonrecurrent group. Conversely, another study suggested that individuals with a PMA < 40° were more likely to achieve complete recovery (21). The reasons for the inconsistent results in prior studies are still unclear; no previous research has been dedicated to exploring the treatment failure of an EBP in patients specifically diagnosed with SIH and concurrent SDH. Nevertheless, our findings indicate that individuals with a smaller PMA, who are diagnosed with SIH and concurrent SDH, may be more likely to treatment failure post EBP. Narrowing the PMA could potentially indicate the extent of brain sagging and caudal displacement of the brainstem (46). Despite successful leak blockage following EBP treatment, resetting the brain becomes increasingly challenging, thereby increasing the likelihood of persistent headache and other discomforting symptoms. This may explain why our results suggest that a smaller PMA is associated with an increased likelihood of treatment failure post EBP in patients with SIH and concurrent SDH.

The strengths of our study lie in its being the first to develop a predictive model for the risk of treatment failure in patients with intracranial hypotension and a SDH following an EBP, utilizing the largest sample size reported thus far. While previous studies have associated hematoma density with an SDH prognosis, our study demonstrates a relationship between hematoma density type and prognosis in SIH-related cases. Our findings suggest that a low-density SDH may be associated with a lower risk of treatment failure in patients with SIH and concurrent SDH. Moreover, the 4 variables integrated into the model—gender, MTH, SDH density type, and PMA—are easy to obtain, cost-effective, and practical for clinical use. Our nomogram demonstrated strong predictive accuracy with a C-index of 0.87 in the development cohort and 0.84 in the validation cohort, highlighting its utility in identifying patients at high risk of treatment failure.

Limitations

Our study has several limitations. First, although it includes the largest sample among similar studies, the overall sample size remains modest. Future multicenter studies with larger and more diverse populations are warranted to confirm and generalize these findings.

The second limitation is the exclusion of SIH cases due to iatrogenic causes and CSF fistulas. As these patients reportedly respond differently to EBP treatment

than those with SIH, the model's applicability to this subgroup is limited (47,48). Refining predictive models may benefit from incorporating advanced imaging techniques, including nuclear medicine cisternography, lateral decubitus digital subtraction myelography, and photon-counting CT myelography, all of which offer high diagnostic accuracy for CSF fistulas and SIH-related features (49).

Another limitation is the reliance on HT2W-MRM for targeted EBP therapy without a reference standard to verify CSF leak localization. Although prior studies suggest that HT2W-MRM-based targeted EBP therapy is more effective than CT myelography-based or blinded EBP for SIH (30,50), its efficacy in patients with a SDH remains unclear. Further research is required to clarify this issue.

Additionally, we included patients who underwent multiple EBP treatments after admission. Although the number of EBP sessions did not significantly differ between treatment failure and nonfailure groups, this factor may introduce bias when applying our model in different populations. Future prospective studies should consider analyzing only first-time EBP recipients to reduce potential bias associated with repeated treatments.

Finally, as a retrospective study, this research requires validation through future randomized controlled trials to confirm its clinical benefits.

Conclusion

Our study developed a model integrating clinical and imaging features to facilitate individualized prediction of EBP treatment failure in patients with SIH and concurrent SDH. This model enables early identification of high-risk patients, emphasizing the need for intensified follow-up to optimize outcomes. Additionally, our findings may provide valuable insights for guiding future clinical practice and translational research.

Ethics/Ethical Approval

This study was approved by the institutional ethics committee of Sir Run Run Shaw hospital, School of Medicine, Zhejiang University (No. 2023-745-01). Given its retrospective nature, the ethics committee waived the requirement for informed consent from patients. The study was conducted in accordance with the Declaration of Helsinki (1964) and its later amendments. No identifiable patient information is included in this manuscript. This research adheres to the 2024 STROCSS criteria for the reporting of cohort studies.

Data Availability

The datasets generated during and/or analyzed during the current study are available from the corresponding author upon reasonable request.

Acknowledgments

We sincerely thank all the patients who participated in this study and completed the follow-up. Their involvement was invaluable in advancing our understanding of treatment outcomes for SIH with concomitant SDH.

Author Contributions

All authors contributed to the study conception and design. Material preparation, data collection, and analysis were performed by Hua Huang, Zhong-Feng Niu, and Fei-Fang He. The first draft of the manuscript was written by Hua Huang and all authors commented on previous versions of the manuscript. All authors read and approved the final manuscript.

References

1. Kranz PG, Gray L, Amrhein TJ. Spontaneous intracranial hypotension: 10 myths and misperceptions. *Headache* 2018; 58:948-959.
2. Chen YC, Wang YF, Li JY, et al. Treatment and prognosis of subdural hematoma in patients with spontaneous intracranial hypotension. *Cephalalgia* 2016; 36:225-231.
3. Schievink WI, Maya MM, Moser FG, Tourje J. Spectrum of subdural fluid collections in spontaneous intracranial hypotension. *J Neurosurg* 2005; 103:608-613.
4. Kelley GR, Burns JD. "Sinking into a coma" from spontaneous intracranial hypotension. *Neurology* 2018; 90:867-868.
5. Albayram S, Kilic F, Ozer H, Baghaki S, Kocer N, Islak C. Gadolinium-enhanced MR cisternography to evaluate dural leaks in intracranial hypotension syndrome. *AJNR Am J Neuroradiol* 2008; 29:116-121.
6. Cirillo L, Verna F, Princiotta C, et al. Spontaneous intracranial hypotension and subdural hematomas treatment management using MMA embolization and target blood patch: A case report. *Life (Basel)* 2024; 14:250.
7. Ferrante E, Rubino F, Beretta F, Regna-Gladin C, Ferrante MM. Treatment and outcome of subdural hematoma in patients with spontaneous intracranial hypotension: A report of 35 cases. *Acta Neurol Belg* 2018; 118:61-70.
8. Healy DG, Goadsby PJ, Kitchen ND, Yousry T, Hanna MG. Neurological picture. Spontaneous intracranial

hypotension, hygromata and haematomata. *J Neurol Neurosurg Psychiatry* 2008; 79:442.

9. Rettenmaier LA, Park BJ, Holland MT, et al. Value of targeted epidural blood patch and management of subdural hematoma in spontaneous intracranial hypotension: Case report and review of the literature. *World Neurosurg* 2017; 97:27-38.
10. Takahashi K, Mima T, Akiba Y. Chronic subdural hematoma associated with spontaneous intracranial hypotension: Therapeutic strategies and outcomes of 55 cases. *Neurol Med Chir (Tokyo)* 2016; 56:69-76.
11. Beck J, Gralla J, Fung C, et al. Spinal cerebrospinal fluid leak as the cause of chronic subdural hematomas in nongeriatric patients. *J Neurosurg* 2014; 121:1380-1387.
12. Schievink WI. Spontaneous spinal cerebrospinal fluid leaks and intracranial hypotension. *JAMA* 2006; 295:2286-2296.
13. Amrhein TJ, Kranz PG, Cantrell S, et al. Efficacy of epidural blood patching or surgery in spontaneous intracranial hypotension: An evidence map protocol. *Syst Rev* 2022; 11:116.
14. Amrhein TJ, Befera NT, Gray L, Kranz PG. CT fluoroscopy-guided blood patching of ventral CSF leaks by direct needle placement in the ventral epidural space using a transforaminal approach. *AJNR Am J Neuroradiol* 2016; 37:1951-1956.
15. Rashid R, Sohrabi C, Kerwan A, et al. The STROCSS 2024 guideline: strengthening the reporting of cohort, cross-sectional, and case-control studies in surgery. *Int J Surg* 2024; 110:3151-3165.
16. Headache Classification Committee of the International Headache Society (IHS) *The International Classification of Headache Disorders, 3rd edition*. Cephalalgia 2018; 38:1-211.
17. Nomura S, Kashiwagi S, Fujisawa H, Ito H, Nakamura K. Characterization of local hyperfibrinolysis in chronic subdural hematomas by SDS-PAGE and immunoblot. *J Neurosurg* 1994; 81:910-913.
18. Pannullo SC, Reich JB, Krol G, Deck MD, Posner JB. MRI changes in intracranial hypotension. Neurology 1993; 43:919-926.
19. Shah LM, McLean LA, Heilbrun ME, Salzman KL. Intracranial hypotension: Improved MRI detection with diagnostic intracranial angles. *AJR Am J Roentgenol* 2013; 200:400-407.
20. Savoiardo M, Minati L, Farina L, et al. Spontaneous intracranial hypotension with deep brain swelling. *Brain* 2007; 130:1884-1893.
21. Levi V, Di Laurenzio NE, Franzini A, et al. Lumbar epidural blood patch: Effectiveness on orthostatic headache and MRI predictive factors in 101 consecutive patients affected by spontaneous intracranial hypotension. *J Neurosurg* 2019; 132:809-817.
22. Choi H, Lee MJ, Choi HA, Cha J, Chung CS. Intracranial structural alteration predicts treatment outcome in patients with spontaneous intracranial hypotension. *Cephalalgia* 2018; 38:323-331.
23. Wu JW, Hseu SS, Fuh JL, et al. Factors predicting response to the first epidural blood patch in spontaneous intracranial hypotension. *Brain* 2017; 140:344-352.
24. Tay ASS, Maya M, Moser FG, Nuno M, Schievink WI. Computed tomography vs heavily T2-weighted magnetic resonance myelography for the initial evaluation of patients with spontaneous intracranial hypotension. *JAMA Neurol* 2021; 78:1275-1276.
25. Zhang YW, Xu WXZ, Lin J, Ding J, Wang X. Comparison of the accuracy between magnetic resonance hydrography and CT myelography in diagnosing of spontaneous intracranial hypotension syndrome. [Article in Chinese] *Zhonghua Yi Xue Za Zhi* 2025; 105:1004-1009.
26. Lutzen N, Beck J, Carlton Jones L, et al. MRI and surgical findings refine concepts of type 2 cerebrospinal fluid leaks in spontaneous intracranial hypotension. *Radiology* 2025; 314:e241653.
27. Hong J, Li X, Wang K, Gao C, He F, Qi X. Comparison of clinical characteristics with spontaneous intracranial hypotension complicated with subdural hematoma between surgical treatment and non-surgical treatment. *Clin Neurol Neurosurg* 2023; 226:107622.
28. Oh AR, Park J, Jeong JS, et al. Risk factors associated with repeated epidural blood patches using autologous blood. *Korean J Pain* 2022; 35:224-230.
29. Park JY, Ro YJ, Leem JG, Shin JW, Oh Y, Choi SS. Predictors associated with outcomes of epidural blood patch in patients with spontaneous intracranial hypotension. *J Clin Med* 2021;10:922.
30. Kim BR, Lee JW, Lee E, Kang Y, Ahn JM, Kang HS. Utility of heavily T2-weighted MR myelography as the first step in CSF leak detection and the planning of epidural blood patches. *J Clin Neurosci* 2020; 77:110-115.
31. Cullum CK, Do TP, Ashina M, et al. Real-world long-term efficacy and safety of erenumab in adults with chronic migraine: A 52-week, single-center, prospective, observational study. *J Headache Pain* 2022; 23:61.
32. Dalby SW, Smilkov EA, Santos SG, et al. Spontaneous intracranial hypotension - Neurological symptoms, diagnosis, and outcome. *Eur J Neurol* 2025; 32:e16579.
33. Lin PT, Hseu SS, Fuh JL, et al. Sex differences in the clinical manifestations and treatment outcomes in a large cohort of spontaneous intracranial hypotension. *Headache* 2024; 64:1298-1308.
34. Gaonkar VB, Garg K, Agrawal D, Chandra PS, Kale SS. Risk factors for progression of conservatively managed acute traumatic subdural hematoma: A systematic review and meta-analysis. *World Neurosurg* 2021; 146:332-341.
35. Miah IP, Tank Y, Rosendaal FR, et al. Radiological prognostic factors of chronic subdural hematoma recurrence: A systematic review and meta-analysis. *Neuroradiology* 2021; 63:27-40.
36. Baucher G, Troude L, Pauly V, Bernard F, Zieleskiewicz L, Roche PH. Predictive factors of poor prognosis after surgical management of traumatic acute subdural hematomas: A single-center series. *World Neurosurg* 2019; 126:e944-e952.
37. Kwon CS, Al-Awar O, Richards O, Izu A, Lengvenis G. Predicting prognosis of patients with chronic subdural hematoma: A new scoring system. *World Neurosurg* 2018; 109:e707-e714.
38. Villagrasa J, Prat R, Diaz JF, Comunas F. Analysis of prognostic factors in adults with chronic subdural hematoma. [Article in Spanish] *Neurologia* 1998; 13:120-124.
39. Bullock MR, Chesnut R, Ghajar J, et al. Surgical management of acute subdural hematomas. *Neurosurgery* 2006; 58:S16-24; discussion Si-iv.
40. Chen HH, Huang CI, Hseu SS, Lirng JF. Bilateral subdural hematomas caused by spontaneous intracranial hypotension. *J Chin Med Assoc* 2008; 71:147-151.
41. Wang J, Zhang D, Gong X, Ding M. Rapid resolution of subdural hematoma after targeted epidural blood patch treatment in patients with spontaneous

intracranial hypotension. *Chin Med J (Engl)* 2014; 127:2063-2066.

42. Liu LX, Cao XD, Ren YM, Zhou LX, Yang CH. Risk factors for recurrence of chronic subdural hematoma: A single center experience. *World Neurosurg* 2019; 132:e506-e513.
43. Yan C, Yang MF, Huang YW. A reliable nomogram model to predict the recurrence of chronic subdural hematoma after burr hole surgery. *World Neurosurg* 2018; 118:e356-e366.
44. Nakamura N, Ogawa T, Hashimoto T, Yuki K, Kobayashi S. Reevaluation on resolving subdural hematoma (author's transl). [Article in Japanese] *Neurol Med Chir (Tokyo)*. 1981; 21:491-500.
45. Lee SH, Lee J, Kim DW, et al. Factors to predict recurrence after epidural blood patch in patients with spontaneous intracranial hypotension. *Headache* 2024; 64:380-389.
46. Signorelli F, Caccavella VM, Giordano M, et al. A systematic review and meta-analysis of factors affecting the outcome of the epidural blood patching in spontaneous intracranial hypotension. *Neurosurg Rev* 2021; 44:3079-3085.
47. So Y, Park JM, Lee PM, Kim CL, Lee C, Kim JH. Epidural blood patch for the treatment of spontaneous and iatrogenic orthostatic headache. *Pain Physician* 2016; 19:E1115-E1122.
48. Shlobin NA, Shah VN, Chin CT, Dillon WP, Tan LA. Cerebrospinal fluid-venous fistulas: A systematic review and examination of individual patient data. *Neurosurgery* 2021; 88:931-941.
49. Madhavan AA, Kranz PG, Brinjikji W, Mark IT, Amrhein TJ. Photon-counting CT myelography for the detection of spinal CSF leaks. *AJNR Am J Neuroradiol* 2025; 46:846.
50. Ahn C, Lee E, Lee JW, Chee CG, Kang Y, Kang HS. Two-site blind epidural blood patch versus targeted epidural blood patch in spontaneous intracranial hypotension. *J Clin Neurosci* 2019; 62:147-154.